IJHSR
ijhighschoolresearch.org
RESEARCH ARTICLE

An Insulin Delivery Patch Pump with 3D Printed Microneedles

Joy Deng

Amity Regional High School, 25 Newton Rd, Woodbridge, CT, 06525, USA; joy.deng0722@gmail.com
Mentor: Zahra Faraji Rad

ABSTRACT: Current insulin pumps, which are serving 200 million diabetics worldwide who require insulin therapy, face critical limitations, including high costs (~$4000), bulky designs, pain associated with hypodermic needles, and occlusion-prone tubing. This project develops a low-cost, painless, and wireless insulin delivery pump by integrating fluids, electronics, and microneedle modules. The fluids module uses a piezoelectric actuator that achieves target flow rates of 0.02 - 3.0 μL/min at 10 - 20 Hz frequencies, demonstrating a linear relationship between frequency and flow rate. The electronics module utilizes Bluetooth components from commercial earbuds, generating 0.4V signals (measured via an oscilloscope), with plans to integrate amplifiers for 40× signal boosting to meet 15V system criteria within $20 cost cap. The microneedle module features two designs: hollow and open microchannel. Computer simulation results showed that the open microchannel design was more resistant to lateral forces. Two hollow microneedles achieved 90% penetration depth under 0.5 N in synthetic skin, meeting insertion force criteria (< 3 N) within the 3.5 × 3.5 mm^2 size constraint. This approximately $30 prototype addresses key limitations through wireless connectivity, painless microneedle delivery, and affordable piezoelectric actuation, potentially improving the quality of life for over 200 million diabetics.

KEYWORDS: Biomedical Engineering, Biomedical Devices, Insulin Pump, Piezoelectricity, Fluids, Electronics.

Introduction

Diabetes is a serious chronic condition where the patient cannot produce enough insulin to regulate their blood sugar. At least 200 million people across the globe require insulin therapy.[1] Basic treatment is through multiple daily injections (MDI). Insulin pumps are the current state-of-the-art treatment method, as they are less painful and more precise than MDIs.[2] Existing insulin pumps consist of a reservoir, a sensor/starter, an actuator, transportation pathways, and a catheter or needle (Figure 1).[3]

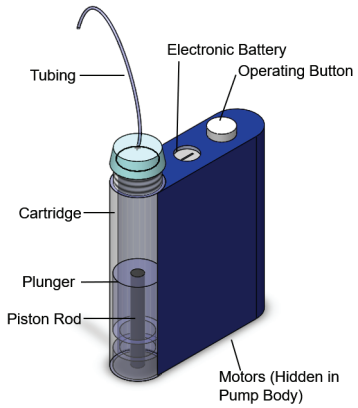

Figure 1: Components of a typical insulin pump.

Yet, existing pumps come with their own problems, including high costs, inconveniently long tubing, fixed dosages, and a large size. These disadvantages not only inhibit freedom of movement and cause insulin waste but can also lead to life-threatening complications, as the tubing can build up pressure and lead to clogging and hyperglycemia.[4] Moreover, even the best insulin pumps on the market are insufficient in flow rates, discreetness, and costs. Table 1 shows a comparison of typical insulin pumps available on the market. Expensive versions, such as Medtronic and Tandem, often feature integratable Continuous Glucose Monitor (CGM) software and extended infusion sets, as seen in Medtronic's case. Medtronic holds a 41.4% market share in the insulin pump market, while Tandem has a 9.2% share, and Insulet's Omnipod has a 16.2% share.[5]

Table 1: Comparison chart of typical insulin pumps on the market and size comparison of a Band-Aid and the fluids module of this project.

	Omnipod DASH	Medtronic Minimed 630G	Tandem Tslim	V-Go	This Project
Cost (w/o insurance)	$600	$3,500	$4000	$635	**$30**
Dimension (mm)	53 x 52 x 10	39 x 98 x 24	51 x 80 x 15	61 x 33 x 13	**40 x 10 x 3**
Actuating Method	Step Motor	Step Motor	Step Motor	Compressed spring	**Piezoelectric**
Tubeless	Yes	No	No	Yes	**Yes**
Adjustable rates	Yes	Yes	Yes	No	**Yes**
Painless Injection	No	No	No	No	**Yes**

In addition, it is important to note that basal treatment of continuous subcutaneous insulin infusion (CSII) works by delivering rapid-acting insulin doses at the set basal rate, unlike that of multiple MDIs, in which long-acting insulin is injected in one go.[6] Therefore, the key to designing an insulin pump is to control basal and bolus rates accurately.

DOI: 10.36838/IJHSR85.83

The inverse piezoelectric effect can effectively achieve this goal, as piezoelectric materials deform elastically under electric fields, enabling each stroke to generate a small but precise displacement.[7] The displacement leads to a pressure change in the pump chamber, and therefore drives the fluid forward. A piezo actuator (such as a piezo buzzer) is thin, typically 0.2 mm in thickness, and inexpensive (around $0.50 apiece), adding to its appeal for insulin micropumps. To engineer a precise micropump, the piezo buzzer's displacement, and hence flow rate, must have a monotonic dependence on the driving signal's amplitude. Previous research showed that the actuation voltage and displacement are approximately proportional within a certain range.[8] Piezoelectric systems are not yet in commercial insulin pumps due to hysteresis leading to actuator fatigue, high sensitivity to air bubbles that can lead to inaccurate dosage, and the general high regulatory burden that requires intensive testing (as piezoelectric pumps are still relatively new).[9] The existing piezoelectric micropumps are too large (80 × 50 × 22 mm) to be a patch pump.[10] Additionally, the complex dual chamber structure is unsuitable for low infusion rates, such as for Type 2 diabetes.[11]

Tubing increases the risk of occlusion, which is the blocking of insulin.[12] Pumps like Medtronic Minimed and Tandem Tslim still have tubing, which limits mobility. Tubing and wires both inhibit freedom of movement. Smart healthcare systems, including wireless monitoring, demonstrate improvements in overall quality of life, particularly in blood sugar management.[13] Therefore, a Bluetooth connection would eliminate the need for wires and would start the pump wirelessly. Just as a mobile phone would send out a signal to earbuds for the speaker to actuate, it also sends out signals to the piezo buzzer at the target frequency and voltage.

Current needles cause pain, while 10% of diabetes patients have needle phobia. Current insulin pumps' infusion sets use hypodermic needles. Typical hypodermic needles are blunt and trigger pain receptors; an alternative option is microneedles. They are extremely sharp and small, so they bypass the stratum corneum barrier of skin without pain.[14] The length of the microneedles is ~ 2.5mm at maximum.[15] The criterion for painless injection is an administrative force of < 3 N.[16] Furthermore, hollow microneedles work well with an auxiliary device.[17] Having open microfluidic channels is new and promising, and easier to manufacture.[18]

Therefore, to engineer a better wireless, discreet, painless, and precise micropump, the goals of this study are to (1) apply the piezoelectric effect to engineering a discreet and precise fluids pump chamber, (2) incorporate wireless electronics that actuate the piezo buzzer on command, and (3) engineer a minimally invasive, painless microneedle patch to deliver liquid.

Methods

Figure 2 shows the overall process and components of the proposed insulin delivery system. First, a mobile phone with data of the target flow rate is sent to the electronics module (Figure 2 [a]). The microprocessor receives the information and sends sinusoidal signals. The signal is amplified by an amplifier to drive the piezo buzzer (Figure 2 [e]), which bends up and down, leading to a change in the volume and pressure of the pump chamber (Figure 2 [d]), therefore activating the fluids module. The fluid is sucked from the reservoir (Figure 2 [c]) and delivered to the end of microneedle patches (Figure 2 [f]), finally exiting to enter the patient's body (Figure 2 [g]).

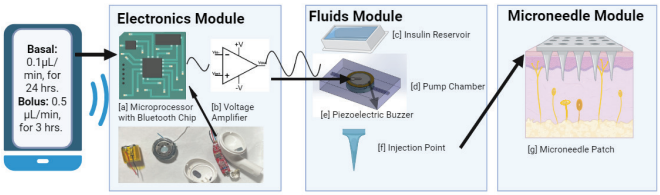

Figure 2: Workflow diagram of insulin pump design, from actuation to insulin entering the patient's body. Created with BioRender.com.

Pump Chamber:

The insulin will travel from the thin reservoir through the actuating chamber with two check valves, layered microfluidic channels, and an outlet (usually a needle) for insulin infusion (Figure 3). The Total Daily Dose (TDD) calculation is usually 0.4 - 1 units per kilogram of bodyweight for Type 1 Diabetics[19] and 0.1 - 0.2 units per kilogram of bodyweight for Type 2 Diabetics.[20] The standard split between basal and bolus rates is 50/50. Therefore, the bolus flow rates will be 0.2 - 3.0 µL/min, based on the floor and ceiling numbers of 4 - 62 units per 3.5 hours for U100 insulin.[21] Therefore, the criterion is a flow rate of 0.02 - 3.0 µL/min.

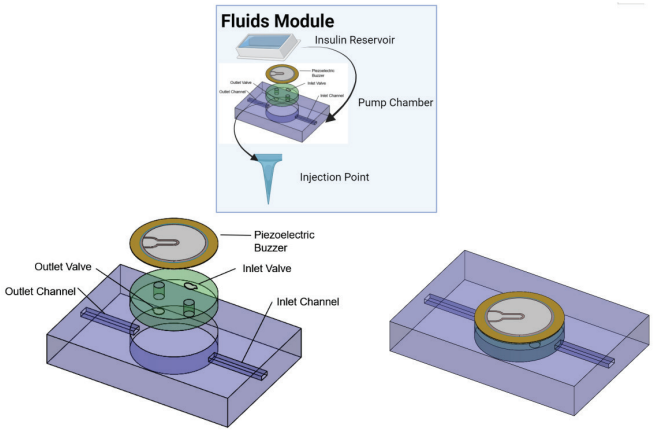

Figure 3: Pump chamber diagram.

(Note: These images are only models to demonstrate the structure of the pump chamber and are not designed to scale; the actual pump chamber is much thinner.)

The actuation amplitude, frequency, and waveform were controlled by the function generator, and the signal was delivered to the piezoelectric buzzer. The flow rate was then observed by tracking the motion of moving specks in the simulated pump chamber. The flow rate was calibrated by placing an object with a known size under the microscope and converting the actual measurements to pixels on screen; therefore, the distance travelled by the fluid was calculated.

After receiving electrical signals, the piezo buzzer (Figure 2 [e]) deforms vertically, leading to a change in the volume and pressure of the chamber (Figure 2 [d]), which causes insulin to enter and exit the chamber through one-way check valves. The pump will reciprocate continuously. In engineering the pump

chamber, it is essential to minimize the volume of the pump to reduce errors; therefore, it is designed in layers. This design will be effective, relatively easy to manufacture, and inexpensive (Figure 4).

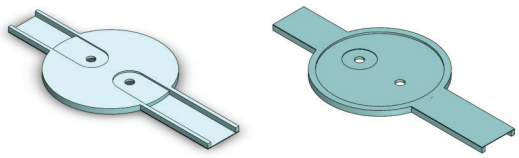

Figure 4: Final pump chamber body and channels design, front and back.

Water was used as the testing liquid because it has approximately the same viscosity as lispro rapid-acting insulin (1.0 mP · s vs. 1.1 mP · s).[21]

The line of motion of water through the pump chamber outlet channel was tracked over time under a microscope to determine the overall flow rate. The micropump's pump chamber, valves, and fluidic channels were made by layers of vinyl cut by a Cricut Joy® Paper Cutter™ (a popular tool among DIYers, which creates layers as thin as 50 µm, finer than most 3D printers can print).

Wireless Electronics:

To establish a connection with mobile phones, a low-cost (~ $10) wireless Bluetooth earbud was directly dissected (Figure 5). Only the actuator would need to be replaced with a typical speaker to a piezo buzzer. So the speaker was cut off, and a piezo buzzer was soldered on. The amplitude and waveform of the signals were measured with an oscilloscope and further adjusted with an amplifier. The criteria were a secure connection with a stable amplitude of 15–20 V (as this was the actuation voltage used to achieve the target flow rate range) and adjustable frequency.

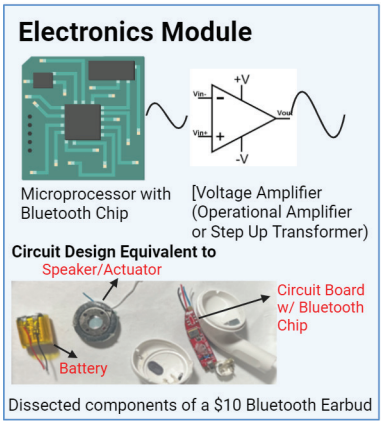

Figure 5: Electronics design further breakdown.

Microneedle Patches:

The microneedle had two designs: hollow and open microchannels (Figure 6) were fabricated by a high-precision 3D printer at Parvus Microstructures LLC (Minnesota, United States) with ~ 20 µm resolution. SOLIDWORKS stress analysis was used as a preliminary test to check the validity of the design and collect data on the various tensile and compressive forces. Empirical testing was later performed by measuring the insertion forces, using weights and synthetic skin for different design types and needle spacing. The criteria were to ensure minimal pain with mechanical stability with an insertion force < 3 N, and needle tip deformation < 250 µm. The constraints were a size of < 3 x 3 mm.

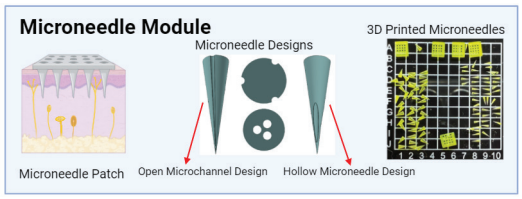

Figure 6 : The microneedle module breakdown.

Results and Discussion

Pump Chamber:

The data indicate an overall linear trend between the frequencies and flow rate (Figure 7). However, the error possibility at 150 Hz is high and might disrupt this conclusion. Currently, frequencies of 10 Hz and 20 Hz satisfy both criteria for a flow rate of 0.02-3.0 µL/min and a frequency below 20 Hz. The final pump chamber design was manufactured using 3 layers of poly-coated paper and had lift check valves to control the direction of flow. This design was mostly successful because it effectively decreased the dynamic load (which is a key factor that limits the performance of piezoelectric pumps) by embedding check valves.[22] However, there were small gaps on the side of the pump chamber formed by uneven adhesive, which likely led to the leakage at the sides when pumping fluid out. Hysteresis and the instability of the input voltage signal might have also contributed to the leakage at < 17 Hz.[23]

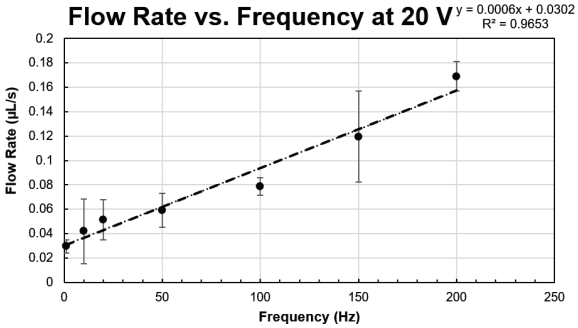

Figure 7: Flow rate vs. actuation frequency in simulated pump chamber, with error bars. There is an overall linear trend between the flow rate and actuation frequency when the voltage is set.

Bluetooth Electronics:

The piezoelectric buzzer was soldered onto the circuit board of the Bluetooth earbud. The Bluetooth earbud was paired and connected with a mobile phone, which was playing a sinusoidal signal using a function generator app. The ends of the Bluetooth earbuds were connected to an oscilloscope, which measured the signal that the Bluetooth earbuds received. This validated the signals the mobile phone was sending out to the Bluetooth earbud, and there was no signal distortion. The amplitude of the initial sinusoidal signal was 0.4 V peak-to-peak, while the target amplitude was 15–20 V; therefore, the signal needed to be amplified. A step-up transformer (which was the original selected amplifier) was soldered between the piezo

DOI: 10.36838/IJHSR85.83

buzzer and microcontroller, but the signal could not be measured because the tension of the clips caused the connection between the transformer and microcontroller to break. This was a limitation in hitting the target voltage, and the amplifying circuit component should be changed. Therefore, future research will focus on switching the Digikey ATB322515-0110 transformer component (3.20mm x 2.50mm x 1.55mm) to a general-purpose operational amplifier, LMV358. However, the concept of dissecting a Bluetooth earbud to act as a controller for the insulin pump system has been validated. The signal before amplification was 20 Hz, with a peak-to-peak voltage of 0.4 V.

Microneedle Patches:

The hollow microneedles were printed out of PMMA and were manufactured accurately as per design (Figure 8). The open microchannel microneedles have had manufacturing issues and have been unable to be inserted. The hollow microneedles have been able to withstand force without large tip deformation while being inserted over 90% into the synthetic skin when each was given a 0.25 N injection force (Figure 9).

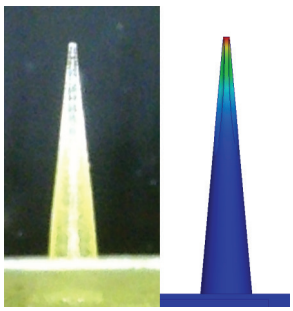

Figure 8: Printed hollow microneedle vs. in simulation.

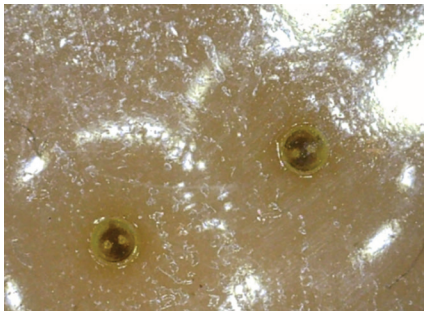

Figure 9: Top view showing hollow microneedles being injected into the skin model.

However, when empirically testing the microneedles, there may have been uncontrolled pressure during handling with tweezers. This could be improved upon by using a precise Universal Tensile Machine, which has been the standard for microneedle testing.[24]

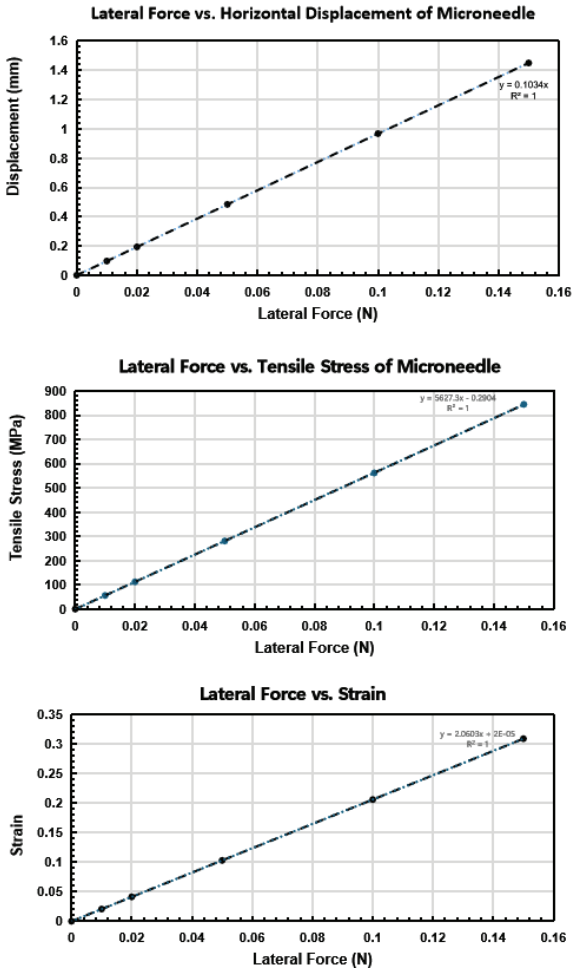

Figure 10: Lateral force vs. horizontal displacement, stress, and strain for open microchannel microneedle. The graphs show a linear relationship between lateral force and the other variables.

The simulation data show that both designs' tip displacement, strain, and stress grew linearly with the applied force (Figure 10). The simulation used a standard mesh in SOLIDWORKS, and forces of 0.01 N, 0.02 N, 0.05 N, 0.10 N, and 0.15 N were applied at the tip of the design, with the base plate fixed. The hollow microneedle previously performed better than the open microchannel microneedle in simulation, but this was due to an error in the positioning of the insertion force. Even then, the vertical tip displacements were very similar (7.16×10^{-3} mm for hollow microneedle vs. 8.82×10^{-3} mm for open microchannel microneedle when 0.125 N vertical force was applied). This was unexpected because it was predicted that the open microchannel microneedle would perform better, as it has more mass and therefore was expected to be more mechanically stable.

Later, the positioning of the forces was adjusted to be identical, and lateral (instead of vertical) forces were applied at the tip, as buckling forces tend to cause more mechanical stress on thin microneedles, especially since the aspect ratio is 1:5 for the designs.

Under the same lateral forces (0.01 N) and material (Polycarbonate), the open microchannel design had a smaller displacement (0.097 mm) than the hollow microneedle (0.113 mm). The same experiment was repeated with two materi-

als-polycarbonate and stainless steel. Polycarbonate is more biocompatible and easier to manufacture than stainless steel, but stainless steel is more rigid than polycarbonate and has a higher elastic modulus. If δ represents the horizontal displacement by the horizontal force, and E represents the material's elastic modulus, then the product of them should be a constant value for the same design, as the force applied is also a constant value. Thus, $k = \delta E/F$, where k is a constant with a unit of m^{-1}. The higher the k is, the more prone the material is to bending. The value k can also be used to calculate the displacement δ when the material and applied force are known. It was calculated that:

$$k_{\text{Hollow Microneedle}} = 2.6 \times 10^7\ m^{-1}$$
$$k_{\text{Open Microchannel Microneedle}} = 2.2 \times 10^7\ m^{-1}$$

Therefore, it can be concluded that the open microchannel microneedle is more rigid. However, these designs show similar k values, so the difference may be within experimental error.

Injecting at a 45-degree angle with the same lateral force resulted in the same horizontal displacement (both 0.97 mm) and in a smaller maximum stress (original was 563 MPa, 45-degree was 562 MPa).

Therefore, lateral forces should be minimized during the injection of the microneedle patch. This includes injecting at an angle or accidental rubbing, as keeping the movement strictly vertical would be ideal for preserving the mechanical shape of the microneedles, minimizing the injection force, and reducing pain.

At 0.1 N lateral force, both microneedle designs displace a significant amount (~ 1 mm), about 1/5 of the total length of the microneedle. More importantly, at a 0.04 mm distance to the tip, the open microchannel microneedle experiences peak stress (56150000 N/m^2), which is close to the maximum tensile strength of the Polycarbonate material (62700000 N/m^2); therefore, the microneedle is close to failure (Figure 11). The safety factor of this design was 1.12 (maximum tensile strength/stress the microneedle experiences). Therefore, the lateral force should be reduced as much as possible, and perhaps in the future, an attachment or fixture to the microneedle patch should be designed to keep the injection motion strictly vertical.

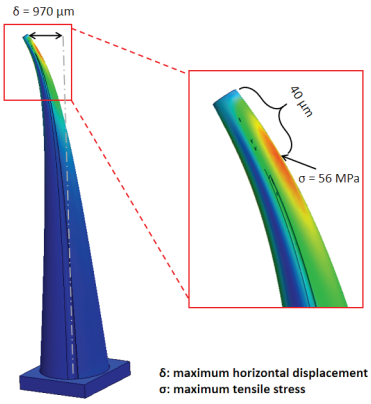

Figure 11: Open microchannel microneedles' displacement and stress under lateral force at the tip under 0.1N lateral force. The microneedle experiences a bending of 0.04 mm from the tip and a horizontal displacement of 0.97 mm.

Conclusion

The purpose of this project was to develop an insulin treatment system for diabetes patients by developing the components of a piezoelectric pump chamber, wireless Bluetooth electronics, and a painless microneedle patch.

The micropump chamber was able to push liquid forward at the target flow rate (0.02 - 3.0 µL/min). The Bluetooth earbud functioned as a complete microcontroller system and successfully actuated the piezoelectric buzzer, similar to System-on-Chip designs.[25] However, it did not hit the target voltage (15 -20V) to successfully actuate the pump yet because numerous attempts to solder on a step-up transformer failed because of the small size of the electronics, and might not have been effective due to core losses and low frequency inefficiency Simulation experimentation of the two microneedle designs showed that the open microchannel microneedle is more resistant to lateral forces, and vertical motion should be maintained through injection. The hollow microneedles were inserted over 90% into the synthetic skin when each was given a 0.25 N injection force.

Table 2: Summary of key metrics & results.

	Flow rate	Wireless actuation	Microneedles
Results	Pump chamber target flow rate (0.02-3.0 µL/min).	Bluetooth earbud signal was 0.4V.	Hollow microneedles were inserted over 90% into the synthetic skin when each was given a 0.25 N injection force.
Limitations	High maintenance of the pump chamber and high fatigue of the valves.	Signal too weak and did not hit the target voltage, substitute with an operational amplifier or other components in the future.	Have not been tested as a microneedle patch.

These three individual components work smoothly, so it is predicted that when integrated, the micropump system has the potential to effectively assist diabetes patients in their treatment. This system has increased discreteness (3 mm thick) and convenience due to the lack of wiring and tubing. The painless microneedles may also lead to an improved experience. The low-cost manufacturing of piezoelectric micropumps has the potential for more affordable and accessible healthcare, saving the healthcare costs of over 11 million Americans. The material cost of the micropump is less than $30, while current pumps cost $700-$3000 without insurance. This micropump has the potential to lower the risk of hyperglycemia and prevent hypoglycemia.

Future research will likely focus on integrating the micropump's three components by amplifying the actuation signal and improving the microneedle patch by adding fixtures. Experiment repeats should also be done to solidify findings.

Acknowledgments

The author thanks Dr.Faraji Rad of University of the Sunshine Coast for being a wonderful mentor, Parvus Microstructures LLC for generously 3D printing microneedles free of charge, and MIT THINK for generously providing funding that supported the continuation of this project.

DOI: 10.36838/IJHSR85.83

References

1. Nkonge, K. M.; Nkonge, D. K.; Nkonge, T. N. Insulin Therapy for the Management of Diabetes Mellitus: A Narrative Review of Innovative Treatment Strategies. Diabetes Therapy **2023**, 14. https://doi.org/10.1007/s13300-023-01468-4.
2. AbdulRasoul, M.; Mousa, M.; Al-Mahdi, M.; Al-Sanaa, H.; Al-AbdulRazzaq, D.; Al-Kandari, H. A Comparison of Continuous Subcutaneous Insulin Infusion vs. Multiple Daily Insulin Injection in Children with Type I diabetes in Kuwait: Glycemic Control, Insulin Requirement, and BMI. Oman Med. J. **2015**, 3 (5), 336–343. https://doi.org/10.5001/omj.2015.69.
3. Paldus, B.; Lee, M. H.; O'Neal, D. N. Insulin Pumps in General Practice. Australian Prescriber **2018**, 41 (6), 186–190. https://doi.org/10.18773/austprescr.2018.056.
4. Hou, M.; Amed, S.; Goldman, R. D. Insulin Pump Complications among Children with Diabetes. Canadian Family Physician **2022**, 68 (12), 893–895. https://doi.org/10.46747/cfp.6812893.
5. Bureau, E. N. *Glucose monitoring app recall risks Tandem's position in insulin pump market: GlobalData*. Express Healthcare. https://www.expresshealthcare.in/news/glucose-monitoring-app-recall-risks-tandems-position-in-insulin-pump-market-globaldata/445291/.
6. Elian, V.; Popovici, V.; Emma-Adriana Ozon; Adina Magdalena Musuc; Ancuța Cătălina Fița; Rusu, E.; Radulian, G.; Dumitru Lupuliasa. Current Technologies for Managing Type 1 Diabetes Mellitus and Their Impact on Quality of Life—a Narrative Review. Life **2023**, 13 (8), 1663–1663. https://doi.org/10.3390/life13081663.
7. Curie, Jacques, and Curie, Pierre (**1881**). "Contractions and expansions produced by voltages in hemihedral crystals with inclined faces," Comptes Rendus 93: 1137-1140.
8. Asadi Dereshgi, H.; Yildiz, M. Z. A Novel Micropump Design: Investigation of the Voltage Effect on the Net Flow Rate. Sakarya Univ. J. Sci. **2018**, 22 (4), 1152–1156. https://doi.org/10.16984/saufenbilder.388658.
9. Axelsson, K.; Mohammadhossien Sheikhsarraf; Kutter, C.; Richter, M. Self-Sensing of Piezoelectric Micropumps: Gas Bubble Detection by Artificial Intelligence Methods on Limited Embedded Systems. Sensors **2025**, 25 (12), 3784–3784. https://doi.org/10.3390/s25123784.
10. Yang, Z.; Dong, L.; Wang, M.; Liu, G.; Li, X.; Li, Y. A Wearable Insulin Delivery System Based on a Piezoelectric Micropump. Sensors and Actuators A: Physical **2022**, 347, 113909. https://doi.org/10.1016/j.sna.2022.113909.
11. Borot, S.; Franc, S.; Cristante, J.; Penfornis, A.; Benhamou, P.-Y.; Guerci, B.; Hanaire, H.; Renard, E.; Reznik, Y.; Simon, C.; Charpentier, G. Accuracy of a New Patch Pump Based on a Microelectromechanical System (MEMS) Compared to Other Commercially Available Insulin Pumps. J. Diabetes Sci. Technol. **2014**, 8 (6), 1133–1141. https://doi.org/10.1177/1932296814543946.
12. Klonoff, D. C.; Freckmann, G.; Heinemann, L. Insulin Pump Occlusions: For Patients Who Have Been Around the (Infusion) Block. J. Diabetes Sci. Technol. **2017**, 11 (3), 451–454. https://doi.org/10.1177/1932296817700545.
13. Dhamanti, I.; Nia, I. M.; Nishara, K.; Srikaanth, B. P. Smart Home Healthcare for Chronic Disease Management: A Scoping Review. Digit. Health **2023**, 9. https://doi.org/10.1177/20552076231218144.
14. Waghule, T.; Singhvi, G.; Dubey, S. K.; Pandey, M. M.; Gupta, G.; Singh, M.; Dua, K. Microneedles: A Smart Approach and Increasing Potential for Transdermal Drug Delivery System. Biomed. Pharmacother. **2019**, 109, 1249–1258. https://doi.org/10.1016/j.biopha.2018.10.078.
15. Aldawood, F. K.; Andar, A.; Desai, S. A Comprehensive Review of Microneedles: Types, Materials, Processes, Characterizations and Applications. Polymers **2021**, 13 (16), 2815. https://doi.org/10.3390/polym13162815.
16. Davis, S. P.; Landis, B. J.; Adams, Z. H.; Allen, M. G.; Prausnitz, M. R. Insertion of Microneedles into Skin: Measurement and Prediction of Insertion Force and Needle Fracture Force. Journal of Biomechanics **2004**, 37 (8), 1155–1163. https://doi.org/10.1016/j.jbiomech.2003.12.010.
17. Oliveira, C.; Teixeira, J. A.; Oliveira, N.; Ferreira, S.; Botelho, C. M. Microneedles' Device: Design, Fabrication, and Applications. Macromol **2024**, 4 (2), 320–355. https://doi.org/10.3390/macromol4020019.
18. Faraji Rad, Z.; Nordon, R. E.; Anthony, C.; Bilston, L. E.; Prewett, P. D.; Arns, J.-Y.; Arns, C. H.; Zhang, L.; Davies, G. High-Fidelity Replication of Thermoplastic Microneedles with Open Microfluidic Channels. Microsyst. Nanoeng. **2017**, 3. https://doi.org/10.1038/micronano.2017.34.
19. Janež, A.; Guja, C.; Mitrakou, A.; Lalic, N.; Tankova, T.; Czupryniak, L.; Tabák, A. G.; Prazny, M.; Martinka, E.; Smircic-Duvnjak, L. Insulin Therapy in Adults with Type 1 Diabetes Mellitus: A Narrative Review. *Diabetes Therapy* **2020**, *11*(2), 387–409. https://doi.org/10.1007/s13300-019-00743-7.
20. Bui, T.-L.; Silva-Hirschberg, C.; Torres, J.; Armstrong, A. W. Hidradenitis Suppurativa and Diabetes Mellitus: A Systematic Review and Meta-Analysis. Journal of the American Academy of Dermatology **2018**, 78 (2), 395–402. https://doi.org/10.1016/j.jaad.2017.08.042.
21. Adams, G. G.; Meal, A.; Morgan, P. S.; Alzahrani, Q. E.; Zobel, H.; Lithgo, R.; Kok, M. S.; Besong, D. T. M.; Jiwani, S. I.; Ballance, S.; Harding, S. E.; Chayen, N.; Gillis, R. B. Characterisation of Insulin Analogues Therapeutically Available to Patients. PLOS ONE **2018**, 13 (3), e0195010. https://doi.org/10.1371/journal.pone.0195010.
22. Zhao, X.; Zhao, D.; Guo, Q. A Theoretical and Experimental Study of a Piezoelectric Pump with Two Elastic Chambers. Sensors **2020**, 20 (20), 5867. https://doi.org/10.3390/s20205867.
23. Rodriguez-Fortun, J. M.; Orus, J.; Alfonso, J.; Buil, F.; Castellanos, J. A. Hysteresis in Piezoelectric Actuators: Modeling and Compensation. IFAC Proceedings Volumes **2011**, 44 (1), 5237–5242. https://doi.org/10.3182/20110828-6-it-1002.01063.
24. Tsuboko, Y.; Sakoda, H.; Okamoto, Y.; Nomura, Y.; Yamamoto, E. Mechanical Characterization of Individual Needles in Microneedle Arrays: Factors Affecting Compression Test Results. Pharmaceutics **2024**, 16 (11), 1480. https://doi.org/10.3390/pharmaceutics16111480.
25. Wang, H. S.; Jambek, A. B.; Bin Abd Aziz, Z. A.; Md Isa, M. N.; Harun, A.; Mohyar, S. N. Design and Implementation of Bluetooth Microcontroller in System-On-Chip (SoC). AIP conference proceedings **2024**, 3050, 030008–030008. https://doi.org/10.1063/5.0192104.

Author

Joy Deng is a Senior at Amity Regional High School and is passionate about innovation in engineering and physics, minorities in STEM, medical care issues, and cultural appreciation.